Acrylonitrile Quenching of Trp Phosphorescence in Proteins: A Probe of the Internal Flexibility of the Globular Fold

Giovanni B. Strambini* and Margherita Gonnelli
Consiglio Nazionale delle Ricerche, Istituto di Biofisica, Pisa, Italy

ABSTRACT Quenching of Trp phosphorescence in proteins by diffusion of solutes of various molecular sizes unveils the frequency-amplitude of structural fluctuations. To cover the sizes gap between O_2 and acrylamide, we examined the potential of acrylonitrile to probe conformational flexibility of proteins. The distance dependence of the through-space acrylonitrile quenching rate was determined in a glass at 77 K, with the indole analog 2-(3-indoyl) ethyl phenyl ketone. Intensity and decay kinetics data were fitted to a rate, $k(r) = k_0 \exp[-(r - r_0)/r_e]$, with an attenuation length $r_e = 0.03$ nm and a contact rate $k_0 = 3.6 \times 10^{10}$ s^{-1}. At ambient temperature, the bimolecular quenching rate constant (kq) was determined for a series of proteins, appositely selected to test the importance of factors such as the degree of Trp burial and structural rigidity. Relative to $kq = 1.9 \times 10^9$ $M^{-1}s^{-1}$ for free Trp in water, in proteins kq ranged from 6.5×10^6 $M^{-1}s^{-1}$ for superficial sites to 1.3×10^2 $M^{-1}s^{-1}$ for deep cores. The short-range nature of the interaction and the direct correlation between kq and structural flexibility attest that in the microsecond-second timescale of phosphorescence acrylonitrile readily penetrates even compact protein cores and exhibits significant sensitivity to variations in dynamical structure of the globular fold.

INTRODUCTION

The study of protein dynamics is drawing attention from the realization that in these biological macromolecules flexibility and function are intimately correlated. Evidence is accumulating to show that slow collective motions in the microsecond-second time domain, underlying transitions between distinct conformational substates, are directly linked to enzyme catalysis, signal transduction and macromolecular recognition (1–5). Notwithstanding the relevance to their biological function, the amplitude-frequency spectrum of slow motions in globular proteins is poorly characterized. In particular, detection of transitions to rarely populated conformational substates, that may be functionally important, still represents an experimental challenge (2,6).

One approach to gather information on the frequencies and amplitudes of structural fluctuations is by the diffusion of small solutes through the macromolecule, a process requiring transient formation of channels or the opening of gates of proportionate size in a generally compact globular fold. A popular method has been to monitor the quenching of the luminescence of internal Trp residues by the penetration of quenching molecules, Q, of various sizes. The technique, initially applied to quenching of Trp fluorescence on the nanosecond time domain (7), has developed its full potential with the less intense, long-lived phosphorescence emission (8–16), as it permits to monitor diffusion rates in the microsecond-second timescale. Quenching studies measure the phosphorescence lifetime, τ, as a function of the quencher concentration, $[Q]$, and evaluate the bimolecular quenching rate constant, kq, from the gradient of the Stern-Volmer plot

$$1/\tau = 1/\tau_0 + kq[Q],$$

where τ_0 is the unperturbed lifetime. For efficient quenching of Trp free in solution kq is close to the diffusion-limited rate constant kd, where $kd = 4\pi r_0 D$ (r_0 is the sum of molecular radii and D the sum of the diffusion coefficients). With Trp residues buried in proteins, kq may fall by several orders of magnitude (10) reflecting, in practice, the extent by which Q diffusion through the protein matrix is slowed down relative to diffusion in water.

For a quenching solute to probe protein dynamics kq must be fully determined by the rate of Q migration through the protein matrix, which is to say that alternative quenching pathways, such as long-range through-space interactions with Q in the solvent, make a negligible contribution to the overall rate. For diffusive migration to be competitive with long-range interactions with Q in the solvent, the quencher needs to be is a relatively small, neutral molecule that interacts with the excited triplet-state of indole only at a short distance range if not by molecular collision. Among known quenchers that conform to this requisite are small diatomic molecules like O_2, NO, and CO, which diffuse readily through globular proteins including most compact cores (13,14,16,17). In proteins, $kq(O_2)$ values are relatively large, and exhibit modest variations between rigid and flexible sites, to indicate that small amplitude fluctuations required for O_2 migration are pervasive of the globular fold. As a consequence of it, O_2 quenching is also found to be insensitive to changes in protein flexibility that may be induced by ligand binding or change in experimental conditions. Larger quenchers, charged and neutral molecules, have also

Submitted April 1, 2010, and accepted for publication May 17, 2010.

*Correspondence: strambini@pi.ibf.cnr.it

Editor: Alberto Diaspro.

0006-3495/10/08/0944/9 $2.00

doi: 10.1016/j.bpj.2010.05.022

been examined (8,16). In general, however, no knowledge is available of the distance dependence of the quenching interaction, $k(r)$, to distinguish between Q penetration and long-distance quenching from the solvent, and often the latter has been suggested to be the prevailing mechanism. One exception is acrylamide, for which the determination of $k(r)$ indicated that through-space quenching makes a negligible contribution to the overall rate when Trp residues are buried a couple of Å below the molecular surface (10). Because of its size, about twice that of O_2, the internal diffusion of acrylamide was found to be slowed down strongly relative to O_2, and to be modulated promptly by binding of ligands or metal ions (10,17). In some proteins the access of acrylamide is regulated by protein gates (15), whereas in some compact protein cores acrylamide quenching is hardly detectable on a second timescale, suggesting that these internal regions are, in practice, impermeable to molecules of this size (10).

To extend the inquiry on the frequency-amplitude spectrum of structural fluctuations to the intermediate amplitude range, this study attempts to cover the gap in Q size between O_2 and acrylamide by examining the potential of acrylonitrile (mol wt = 53) to probe protein dynamics. Acrylonitrile (AN) is a neutral molecule with a π-electron configuration similar to acrylamide, which presupposes a comparable short-range interaction with the indole triplet-state and protein quenching mechanism. We report quenching experiments carried out to: 1), evaluate the distance range of through-space interactions between AN and model indole compounds, both in low-temperature rigid glasses and in fluid solutions; 2), evaluate kq(AN) for a set of proteins with increasing degree of Trp burial; and 3), test for a possible correlation between kq(AN) and changes in structural flexibility induced by metal binding to apo-proteins or complex formation with coenzymes and analogs. To make a full comparison between kq(AN) and kq(acrylamide), acrylamide quenching rate constants were also determined for those proteins among the current set for which kq(acrylamide) had not been determined before.

MATERIALS AND METHODS

All chemicals were of the highest purity grade available from commercial sources and unless specified to the contrary were used without further purification. *N*-acethyltryptophanamide (NATA) was from Sigma-Aldrich (St. Louis, MO) and before use was recrystallized twice from ethanol/water. 2-(3-Indoyl) ethyl phenyl ketone (IEPK), prepared according to the procedure of Tamaki (18), was a gift from Dr. Lee (Department of Chemistry, McGill University, Montreal, Canada). NAD^+, ADPR, pyrazole, and acrylonitrile (99%) were from Sigma-Aldrich. Acrylamide (99.9% electrophoretic purity) was from Bio-Rad Laboratories (Richmond, CA). Tris (hydroxymethyl)-aminomethane (Tris) and NaCl Suprapur were from Merck (Darmstadt, Germany). Water was purified by reverse osmosis (Milli-RX 20; Millipore, Billerica, MA) and subsequently passed through a Milli-Q Plus system (Millipore).The proteins horse liver alcohol dehydrogenase (LADH), alkaline phosphatase (AP) from *Escherichia coli*, and β-lactoglobulin A were purchased from Sigma-Aldrich. Ribonuclease T_1 ($RNase\ T_1$) was a gift of Professor C. Nick Pace (Texas A&M University, College Station, TX). Glyceraldehyde-3 phosphate-dehydrogenase (GAPDH) from *Bacillus stearothermophilus* was kindly supplied by Professor G. Branlant, University Henri Poincaré (Nancy, France). Wild-type azurin from *Pseudomonas aeruginosa* was prepared from the plasmid carrying the wild-type sequence, supplied by Professor A. Desideri (Università di Roma, Tor Vergata), after a procedure analogous to that described by Karlsson et al. (19). The azurin mutant C112S was prepared after the same procedure as for the wild-type protein except for the omission of any $CuSO_4$ addition in both growth and purification medium. The C112S mutant was constructed using the QuikChange kit (Stratagene, La Jolla, CA) and confirmed by sequencing.

The complexes of LADH (8 μM) with ADPR and with NAD^+ plus pyrazole were formed simply by adding the reagents to the protein solution to a final concentration of 430 μM for ADPR, 9 μM for NAD^+, and 10 mM for pyrazole. To remove NAD^+ from GAPDH the enzyme was treated with activated charcoal as reported before (20). The GAPDH/NAD^+ complex was formed by adding 44 μM NAD^+ to 4 μm GAPDH. Copper-free azurin (apo-azurin) was prepared from holo-azurin by adding 0.1 M potassium cyanide and 1 mM EDTA in 0.15 Tris-HCl, pH 8, followed by column chromatography (21). Zn-azurin was formed from apo-azurin by the addition of $ZnCl_2$ in the molar ratio 2:1 (22). mdAP is a Zn-depleted form of AP prepared by dialysis of the native protein in the presence of 20 mM EDTA for 3 h, followed by dialysis with pure buffer. Full recovery of native AP, as monitored by the characteristically long phosphorescence lifetime, was obtained within an hour of incubating mdAP in 2 mM $ZnCl_2$.

AN and acrylamide stocks solutions used in quenching experiments were prepared daily, by diluting the commercial supply in the same buffer used with each protein system (Table 1). The buffer was 20 mM Tris-HCl, pH 7 or 7.5, 30 mM sodium acetate + 1 mM EDTA, pH 5.5 and 30 mM potassium phosphate, pH 7.

For measurements in low-temperature (77 K) glasses, IEPK (2×10^{-3} M) solutions in absolute ethanol, containing varying concentrations of AN, were placed in Spectrosil quartz tubing (4 mm inside diameter) and closed off from the atmosphere. To avoid the formation of cracks in the glass, the samples were gradually cooled to near liquid N_2 temperature before their immersion in a liquid N_2 containing Dewar. The steady-state phosphorescence intensity, on excitation at 292 nm, was corrected for the weak absorption of AN (A_{292}) at that wavelength by the factor $-\log(A_{292}/2)$ (23).To correct for the volume contraction of the solution on cooling from 293 to 77 K the room temperature [AN] concentration was multiplied by 1.2.

For phosphorescence measurements in fluid aqueous solutions, NATA and protein samples were placed in appositely constructed, 5×5 mm^2, quartz cuvettes with a leak proof capping designed to allow thorough removal of O_2, either by the alternating application of moderate vacuum and inlet of ultrapure N_2 (24) or by means of an enzymatic deoxygenating system (25). Enzymatic deoxygenation was adopted in AN quenching experiments because, AN being moderately volatile, repeated application of vacuum would tends to decrease its concentration in solution. To reduce the time and improve the efficiency of enzymatic deoxygenation, the samples were briefly (2 min) degassed by vacuum pump/N_2 exchange before the addition of the AN aliquot. Subsequently, the AN aliquot was introduced by opening the cap under N_2 atmosphere. In this way satisfactory deoxygenation, at ambient temperature, was achieved in ~8 min. The enzymatic system consisted of glucose oxidase (0.2 μM), catalase (0.04 μM) and glucose (0.3%). The reduction in the phosphorescence lifetime induced by AN was fully reversible on removal of AN by dialysis.

In phosphorescence measurements, the final protein concentration ranged between 2 and 10 μM, unless otherwise specified.

Phosphorescence measurements

A conventional, homemade instrument was used for steady-state phosphorescence intensity measurements in glasses at 77 K. The excitation (292 nm) provided by a Cermax xenon lamp (LX 150 UV; ILC Technology,

TABLE 1 Acrylonitrile phosphorescence quenching rate constants (*kq*) for NATA and for internal Trp residues in selected proteins at 25°C

Sample	Buffer/pH	Trp	τ_0 (ms)	kq ($M^{-1}s^{-1}$)	$\Delta H^{\pm}(kq)$ (kcal/mol)	r_p (nm)	$kq(r_p)$ ($M^{-1}s^{-1}$)
NATA	Tris/7	—	2	1.9×10^9	—	—	—
RNaseT1	NaAc/5.5	59	23	2.9×10^6	5.0	0.2	1.1×10^5
β-lactoglobulin A	NaAc/5.5	19	35	9.6×10^5	10.2	0.25	2.3×10^4
LADH	Tris/7	314	420	4.1×10^5	12.2	0.45	3.6×10^1
LADH/ADPR	Tris/7	314	980	1.2×10^5	14.9	0.45	3.6×10^1
LADH/NAD/pyr	Tris/7	314	510	1.1×10^5	14.0	0.45	3.6×10^1
GAPDH	K Phos/7	84	55	6.2×10^6	13.2	0.5	7.2×10^0
GAPDH/NAD	K Phos/7	84	24	6.5×10^6	12.2	0.5	7.2×10^0
C112S-azurin	Tris/7.5	48	290	5.7×10^3	14.1	0.8	4.1×10^{-4}
WT-apo-azurin	Tris/7.5	48	340	5.1×10^3	13.4	0.8	4.1×10^{-4}
WT-azurin(Zn)	Tris/7.5	48	320	$3.1 \times x10^3$	12.2	0.8	4.1×10^{-4}
AP	Tris/7.5	109	1420	1.36×10^2	16.5	1.1	2.3×10^{-7}
md-AP	Tris/7.5	109	20	9.82×10^2	16.4	1.1	2.3×10^{-7}

Theoretical estimates of the through-space rate, $kq(r_p)$, based on $k(r)$ and on crystallographic data (r_p), is also included.

Sunnyvale, CA) was selected by a 0.25 m monochromator (Jobin-Ivon, H25), and the emission, collected at 90° from the excitation, was dispersed by a 0.3 m triple grating imaging spectrograph (SpectraPro-2300i; Acton Research, Acton, MA) set to a band pass of 2.0 nm. The emission intensity was monitored by a back-illuminated 1340 × 400 pixels CCD camera (Princeton Instruments Spec-10:400B (XTE); Roper Scientific, Trenton, NJ) cooled to −60°C. Excitation and fluorescence light were eliminated from the detection system by a mechanical chopper.

Phosphorescence decays were measured with pulsed excitation on a home made apparatus described before (24). All phosphorescence decays were analyzed in terms of discrete exponential components by a nonlinear least-square fitting algorithm (DAS6; Horiba Jobin Yvon, Milano, Italy).

Quenching experiments in fluid solutions

Acrylonitrile and acrylamide quenching experiments in fluid solutions were carried out by measuring the phosphorescence lifetime, τ, of NATA and proteins samples as a function of the quencher concentration [Q] in solutions (10). The bimolecular quenching rate constant, kq, was derived from the gradient of the Stern-Volmer plot

$$1/\tau = 1/\tau_0 + kq[Q], \tag{1}$$

where τ_0 is the unperturbed lifetime. The phosphorescence decay of some proteins, namely LADH, GAPDH, and β-lactoalbumin, are intrinsically heterogeneous and tend to remains so even when the average phosphorescence lifetime is reduced markedly by AN or acrylamide quenching. Because in all the proteins examined the emission is due to a single Trp residue per subunit, such lifetime heterogeneity reflects the presence of more than one stable conformation of the macromolecule (26), each with its distinct τ_0 and quenching rate constant. For convenience, and also because an evaluation of individual quenching rates is model dependent, lifetime Stern-Volmer plots were all constructed from the intensity averaged lifetime (27) ($\tau_{av} = \sum \alpha_i^2 \tau_i / \sum \alpha_i \tau_i$), obtained in general from a biexponential fit of phosphorescence decays. Thus, the value of kq derived from the gradient of these plots is an average quantity.

For each quencher concentration at least three independent samples were analyzed and the reported results represent the mean lifetime value. The reproducibility of phosphorescence lifetime measurements was generally >5%.

Quenching models

Quenching of the luminescence of buried Trp residues in proteins by small solutes (Q) in solution has been analyzed in terms of mechanisms that involve either Q diffusion to the protein surface followed by long-range interactions with the buried chromophore or diffusive penetration of Q through the protein matrix to its proximity. Pertinent analytical expressions for the quenching rate, obtained by solving Fick's diffusion equation applying radiation boundary conditions, and their application range in the realm of protein phosphorescence have been discussed in detail before (28). Briefly, by neglecting a transient time-dependent term arising from Q molecules already in proximity of the chromophore at the instant of excitation, the steady-state bimolecular quenching rate constant, kq, is given by

$$kq = k_D k_I/(k_D + k_I), \tag{2}$$

where $k_D = 4\pi aD$ is the Smoluchowski diffusion controlled rate constant, $k_I = 4\pi a^2 B$ is the diffusion independent maximum rate constant and D is the sum of the separate diffusion coefficients of Q and protein in solution. B is an interaction strength parameter related to the distance dependence of the quenching interaction, $k(r)$, and a is the distance (center-to-center) of closest approach between Q and chromophore. Depending on which of the two rate constants is smaller the process goes from the diffusion controlled regime ($k_D << k_I$, $kq\ \alpha\ D$) to the reaction controlled regime ($k_D >> k_I$, $kq = k_I$) where kq is independent of diffusion.

External quenching of protein phosphorescence in ordinary aqueous solution by Q relegated to the aqueous phase is believed to fall within the latter regime, owing to the long lifetime of the excited triplet-state and the generally weak, short-range nature of its interactions with Q (8,9). For an exponential electron exchange interaction, $k(r) = k_0 \exp[-(r - r_0)/r_e]$, it was shown that the bimolecular rate constant, assuming an essentially flat protein surface, decreases exponentially with the thickness of the protein spacer (r_p) separating the chromophore from the aqueous interface ($r_p + r_0 = a$ is the shortest center-to-center distance between the internal chromophore and Q at the aqueous interface) according to Vanderkooi et al. (29)

$$kq(r_p) \approx k_I(r_p) = 2\pi N\, 10^{-3}\left[(r_p + r_0)r_e^2 + 2r_e^3\right] \times k_0 \exp(-r_p/r_e)\,M^{-1}s^{-1}, \tag{3}$$

where N is Avogadro's number and r_e is the attenuation length (units of r_e and r_p in cm).

Alternatively, for diffusive penetration of Q across a protein shell of thickness T, characterized by a diffusion constant $D_p << D$, the process is bound to be under diffusion control and in such cases the rate constant assumes the form of a corrected Smoluchowski equation (28)

$$kq = 4\pi a D_p(1 + a/T), \tag{4}$$

where now a is the radius of the impermeable protein core surrounding the chromophore.

Equation 2, Eq. 3, and Eq. 4, contemplate a linear dependence of the quenching rate on [Q], i.e., a linear lifetime Stern-Volmer plot.

RESULTS

AN quenching of IEPK phosphorescence a glass matrix

AN quenches both fluorescence and phosphorescence of indole derivatives. To study selectively the interaction between AN and the excited triplet-state of indole, quenching of the precursor fluorescent state must be avoided. For this, an indole derivative that exhibits only phosphorescence emission was used. That is accomplished with IEPK, a conjugate indole compound with an effective intersystem crossing quantum yield of 1 (18).

The phosphorescence emission (λex = 292 nm) of IEPK (2×10^{-3} M) was monitored in an ethanol glass at 77 K as a function of AN concentration, c. The decrease in steady-state intensity of IEPK, $P(c)/P(0)$, as a function of [AN] is reported in Fig. 1. Before interpreting the data in terms of long–distance indole-AN interactions, quenching by ground-state complex formation must be ruled out. Under these experimental conditions, there is no evidence of ground-state complex formation. At the highest concentration used both absorption (at 20°C) and phosphorescence spectrum (at 77 K) are not affected by the quencher, suggesting that strong ground-state and excited-state complexes

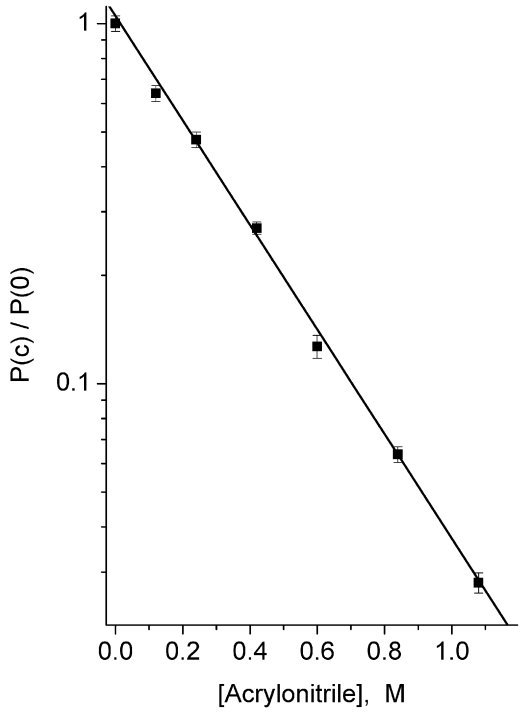

FIGURE 1 Relative phosphorescence yield of IEPK as a function of acrylonitrile concentration in an ethanol glass, at 77 K (steady-state excitation at 292 nm). The concentration of IEPK was 2×10^{-3} M. The intensity values are averages of three separate runs; error bars indicate the range.

are not formed. Additionally, whereas an exponential dependence of $P(c)/P(0)$, as observed here (Fig. 1), is consistent with a random chromophore-quencher distance/orientation, static quenching by dark complexes is predicted to follow a Stern-Volmer concentration dependence (30).

Assuming a random indole-AN distance distribution, we shall interpret the decrease in phosphorescence yield in terms of Perrin's active sphere model (30,31)

$$P(c)/P(0) = \exp(-cv), \tag{5}$$

$$v = (4\pi/3)\left(r_q^3 - r_0^3\right), \tag{6}$$

where c is the quencher concentration (number/volume), v is the volume of the active sphere, $r_0 = (r_{indole} + r_{AN})$ is the sum of the average molecular radii, and r_q is the average center-to-center distance at which the rate of quenching is equal to the unperturbed phosphorescence lifetime, τ_0.

When r_0 is set to 0.5 nm (32), the slope of the semilogarithmic plot yields $r_q = 1.13$ nm.

The phosphorescence decay (λ_{em} = 405–445 nm) of IEPK at 77 K, on pulsed laser excitation at 292 nm, is essentially exponential, and except for a 5–6% short-lived component from solvent impurities, the lifetime τ_0 is 5.2 s. With the addition of AN the decay becomes shorter lived and highly nonexponential. Representative decays as a function of c, solvent-subtracted and normalized by the intensity of IEPK control, $P(c)/P(0)$, are shown in Fig. 2. We also note that the lifetime shortening accounts completely for the quenching of the steady-state intensity as the area under the decay curves follows closely the decrease in phosphorescence yield determined in steady-state measurements.

In rigid media, lifetime shortening and heterogeneous decays are consistent with a quenching interaction that extends beyond van der Waals contact and a distribution of quencher-chromophore geometrical arrangements. The decays $P(c)/P(0)$ were fitted assuming an exponential distance dependence of the quenching rate, $k(r)$, a dependence typical of both electron-transfer (33) and electron exchange interactions (34). Namely,

$$k(r) = k_0 \exp[-(r - r_0)/r_e], \tag{7}$$

where k_0 is the maximum rate at the contact distance r_0 and r_e is the attenuation length. For a random distribution of chromophore-quencher distances, and assuming that the strong dependence on separation determines the distribution of rates (i.e., orientation effects neglected), Huddelston and Miller (35) derived an expression that is applicable to the decay of phosphorescence, in the form

$$P(c)/P(0) = \exp\left\{-\left(4\pi/3\right) c \left[\left(r_0 + r_e \ln(g\, k_0\, t)\right)^3 - r_0^3\right]\right\}, \tag{8}$$

where g is a numerical factor equal to 1.9. Setting r_0 = 0.5 nm, the above expression gave reasonable god fits of

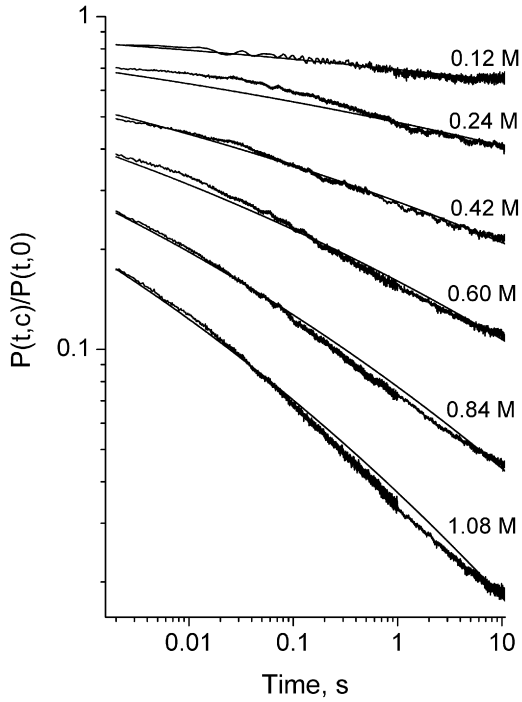

FIGURE 2 Decay of IEPK phosphorescence (λex = 292 nm), in ethanol glass at 77 K, at increasing acrylonitrile concentrations. To enhance the time resolution, the phosphorescence intensity from the same exciting pulse was acquired in two separate timescales and then the data joined into a single intensity-time profile. All intensities $P(c,t)$ are normalized by the control sample $P(t,0)$. The full lines represent the best fit of the data to Eq. 8 with the parameters $r_0 = 0.5$ nm, $r_e = 0.03$ nm, and $k_0 = 2.9 \times 10^8$ s^{-1}. Other experimental conditions are as in Fig. 1.

the phosphorescence data (Fig. 2) with $k_0 = 2.9 \times 10^8\ s^{-1}$ and $r_e = 0.03$ nm. With this distance dependence of the rate, $k(r) = 2.9 \times 10^8 \exp[-(r - 0.5)/0.03]$, the equality $k(r_q) = 1/\tau_0 = 1/5.2\ s^{-1}$ predicts an average transfer radius of 1.13 nm, in full agreement with 1.13 nm obtained from steady-state measurements. In a previous report (10) analogous experiments conducted with acrylamide as a quencher yielded $k_0 = 1.8 \times 10^8$ s^{-1} and $r_e = 0.029$ nm, indicating a distance dependence of the quenching interaction very similar to that found here for AN.

AN quenching of NATA phosphorescence in fluid aqueous solutions

The effectiveness of AN as a quencher of indole phosphorescence in aqueous solutions (10 mM Tris buffer, pH 7), at 25°C, was investigated with the Trp derivative NATA. The addition of AN to a solution of NATA (5×10^{-5} M) shortened the phosphorescence lifetime, maintaining the decay exponential throughout. The decrease of τ as a function of [AN] yielded a linear Stern-Volmer plot (Fig. S1 in the Supporting Material) from which a bimolecular quenching rate constant $kq = 1.9 \times 10^9$ M^{-1}s^{-1} is obtained. This value, which is very similar to 1.67×10^9 M^{-1}s^{-1} obtained for acrylamide at 20°C(10), is smaller than the diffusion rate constant ($\approx 10^{10}$ M^{-1}s^{-1}), presumably owing to the spin statistical factor (36).

AN quenching of Trp phosphorescence in proteins

Protein systems and experimental conditions were selected to provide varying degrees of burial of the phosphorescence probe as well as a wide range of structural flexibility of the Trp site, as inferred from the magnitude of the intrinsic phosphorescence lifetime (37) or from the quenching rate constant of oxygen and acrylamide (10,14,17). The protein examined, their τ_0 at 25°C, and the thickness of the protein spacer, r_p, separating the indole ring from the solvent, as reported by the crystallographic structure, are listed in Table 1. To get a rough estimate of the activation barrier to AN quenching, measurements were extended to supercooled solutions, at −5°C.

Representative Stern-Volmer plots for RNase T1, GAPDH, LADH, and AP are shown in Fig. 3. Throughout, up to the limit of measurable quenching rates, $(1/\tau - 1/\tau_0) \approx 10^4$ s^{-1}, the plots were found to be linear on [AN] (no saturation effects were observed, in contrast with acrylamide quenching of LADH and azurin (10,15)). For this set of proteins the magnitude of kq, obtained from the gradient of these plots (Table 1), shows wide variability, ranging from 6.5×10^6 M^{-1}s^{-1} for the GAPDH/NAD$^+$ complex to ~10^2 M^{-1}s^{-1} for the most deeply buried Trp^{109} of AP. If exception is made for Trp^{84} of GAPDH, that despite being relatively internal is most readily quenched, we note a trend of decreasing kq with the depth of burial, as if the dependence of kq on r_p indicated that the friction to AN diffusive penetration increases the more internal is the site hosting the chromophore.

Fig. 3 and Table 1 also emphasize that binding of NAD$^+$ or ADPR to LADH and removal of Zn^{2+} from azurin and from AP changes significantly the magnitude of kq. In each case we note that the change is directly correlated to alterations in flexibility (and thermal stability) of the macromolecule. In the case of LADH, the ~3.5-fold reduction of kq on complex formation with NAD$^+$ plus pyrazole or with the coenzyme analog ADPR is accompanied by an increases in both τ_0 (38) and thermal stability of the protein (39), changes that are consistent with an enhanced rigidity of the macromolecule. Likewise, the 1.6- and 7-fold enhancement of kq with azurin and AP, respectively, in the transition from holo- to apo-protein after Zn^{2+} removal is associated to a significant drop in the thermal unfolding temperature (40), and of τ_0 in AP, again indicative of a more flexible and unstable fold for the apo-protein. By contrast, little if any change of kq was found for the NAD$^+$ complex of GAPDH, regardless of the greater thermal stability of the latter (41).

Last, the activation enthalpy for the quenching rate constant (Table 1), $\Delta H^{\pm}(kq)$, derived from a two points Arrhenius plot exhibits an abrupt twofold increase from

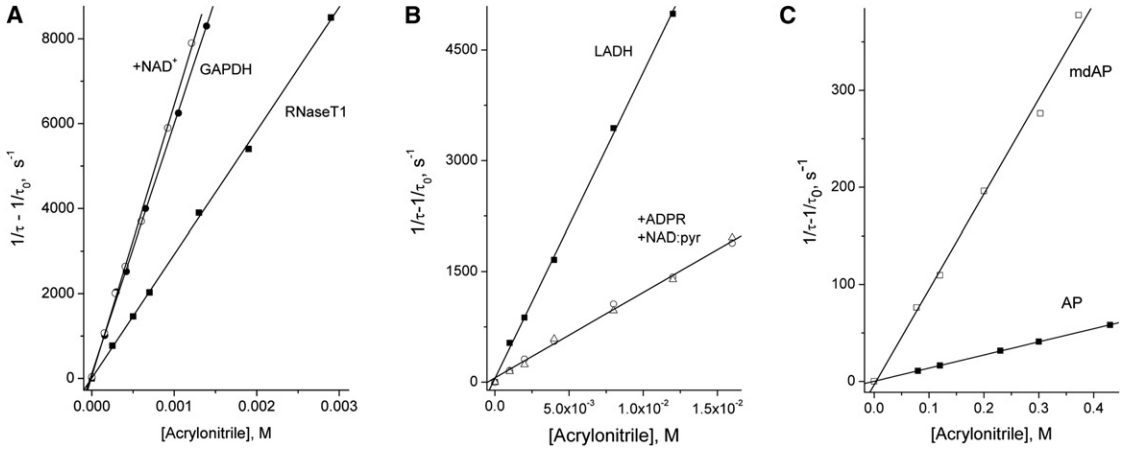

FIGURE 3 Examples of lifetime Stern-Volmer plots relative to the quenching of Trp phosphorescence in various proteins. (*A*) RNaseT1 (■) and GAPDH (●). The open symbols (●) refer to the GAPDH/NAD^+ complex. (*B*) LADH (■) and its binary and ternary complexes with ADPR (○) and NAD/pyrazole (Δ). (*C*) AP (■) and its metal depleted form (mdAP) (□). Buffer conditions and τ_0 are reported in Table 1.

5 kcal/mol for RNase T1, where Trp is nearest to the aqueous interface, to 10 kcal/mol for β-lactoglobulin whose Trp residues is slightly more internal. With the other proteins $\Delta H^{\pm}(kq)$ ranges between 12 and 16.5 kcal/mol with a tendency to increase with slower quenching rates. Apparently, structural fluctuations permitting internal AN diffusion not only decrease in frequency toward the protein interior but are also characterized by higher energy barrier.

DISCUSSION

In the submillisecond-second timescale of phosphorescence, AN was found to readily quench the emission of solvent inaccessible Trp residues in proteins, deep down to compact cores. In principle, the process could be dominated either by long-range interactions with AN in the solvent or by its rapid penetration to the vicinity of the chromophore. Based on the relatively steep distance dependence of the quenching interaction it may be shown that, unless the indole ring is very superficial, through-space quenching makes a negligible contribution to the experimental rate.

Through-space quenching of Trp phosphorescence in proteins by AN

In each protein the impact of through-space interactions can be assessed by applying Eq. 3, with the distance dependence of the reaction, $k(r)$, as derived with model indole compounds in glasses and in liquid solutions. The reaction predictably involves an electron exchange or electron transfer process (8,32), and indeed, the expected exponential dependence of $k(r)$ (33,34) was found to fit adequately AN quenching of IEPK phosphorescence in glasses. At 77 K, the fitting parameters yielded an average interaction radius of 1.13 nm and a rate $k(r) = 2.9 \times 10^8 \exp[-(r - 0.5)/0.03]\ s^{-1}$, confirming that the interaction between the excited triplet-state of indole and AN goes beyond van der Waals contact. The above determination of $k(r)$ refers to a rigid matrix at 77 K. According to theory of Marcus and Sutin (33), electron-transfer rates can be affected by temperature and solvent relaxation, their effects being predominant on the preexponential term, k_0. The variation of k_0 from low temperature glasses to ambient temperature liquids (when quenching in solution is less than diffusion control, $kq < k_D$) can be estimated from the bimolecular quenching rate constant, kq, in these media, applying Eq. 2 in combination with the theoretical expression for k_I pertaining to spherical symmetry (42)

$$k_I = kq\, k_D/(k_D - kq) = 4\pi N 10^{-3}\left[r_e r_0^2 + 2r_e^2 r_0 + 2r_e^3\right] k_0\ M^{-1}s^{-1}, \quad (9)$$

where N is Avogadro's number and distances are in cm. From $kq = 1.9 \times 10^9\ M^{-1}s^{-1}$, obtained for the quenching of NATA phosphorescence in aqueous solutions at 25°C, $k_D \approx 10^{10}\ (M^{-1}s^{-1})$ (43), $r_e = 0.03$ nm and $r_0 = 0.5$ nm one obtains $k_I = 2.3 \times 10^9 = (0.0636)\ k_0\ M^{-1}s^{-1}$, and $k_0 = 3.6 \times 10^{10} s^{-1}$. With this correction, the distance dependence of the quenching reaction at 25°C becomes $k(r) = 3.6 \times 10^{10} \exp[-(r - 0.5)/0.03)]\ s^{-1}$.

Dynamic quenching of internal Trp residues in proteins by AN in the solvent can now be calculated from $k(r)$ and the minimum thickness of the protein spacer, r_p, separating the chromophore from the aqueous interface. The magnitude of $k_I(r_p)$ obtained applying Eq. 3 is compared to the experimental rate constant in Table 1 and is displayed in Fig. 4. For RNase T1, which has the most superficial Trp residue of the proteins list, k_I is 30-fold smaller than kq. The disparity between k_I and kq increases further with the depth of burial, proving that AN quenching from the solvent is expected to make a negligible contribution to the rate, throughout. It should be pointed out that, in contrast to AN, acrylamide quenching from the solvent may sometimes compete and dominate over quencher penetration pathways. The comparison between the observed kq(acrylamide) of

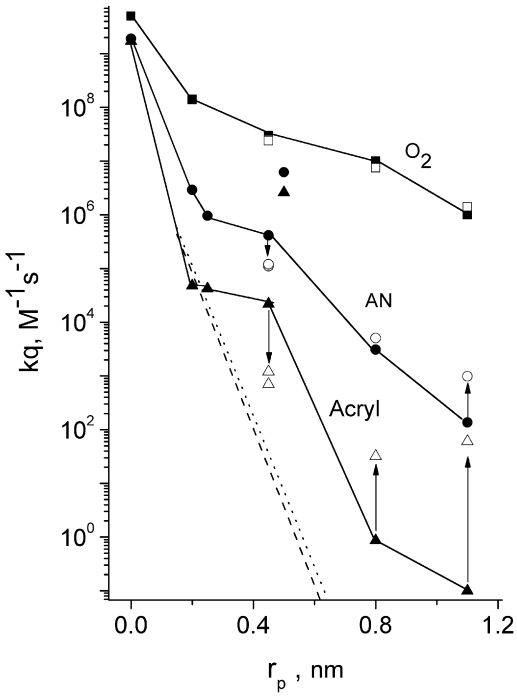

FIGURE 4 Comparison among the bimolecular quenching rate constants of acrylonitrile (•), O_2 (■) and acrylamide (▲) for the proteins of Table 1 (O_2 data is from (14,17) and is not available for β-lactoglobulin and GAPDH. Acrylamide quenching constants were from (10,17) and those for GAPDH, GAPDH/NAD^+ and mdAP were determined in this study). Arrows pointing to open symbols indicate modulation of the respective rate constants by coenzyme/coenzyme analog in LADH and GAPDH, and by Zn removal from azurin and AP. The theoretical rate constant for through-space quenching by Q in the solvent, predicted by Eq. 3 as a function of the distance between the phosphorescence probe and the protein surface (r_p), is shown for both acrylonitrile (*dotted line*) and acrylamide (*dashed line*). Lines joining the points only serve to guide the eye.

these proteins (10,17) and the respective through-space quenching rate constant obtained by the procedure above (Fig. 4) shows that for superficial sites, such as with RNase T1 (and also Ca-parvalbumin, $r_p = 0.25$ nm, G. Strambini and M. Gonnelli, unpublished data) $kq \approx k_I$, implying that in these cases acrylamide quenching may be entirely from the solvent (data confirming external quenching by acrylamide is to be published, G. Strambini and M. Gonnelli, unpublished). Thus, although the through-space rate is very similar between AN and acrylamide, with the larger quencher external quenching may become competitive owing to the strong reduction of the penetration rate with increasing quencher size. Through-space quenching will ultimately limit the size of quenching molecules that can be used in studies of protein dynamics.

AN quenching of Trp phosphorescence and the internal flexibility of the globular fold

Having ruled out long-range interactions with AN in the solvent, two other mechanisms need to be considered for quenching of internal Trp residues. These are, migration of the quencher through the protein matrix to within interaction distance of the indole ring, and, transient local unfolding or large amplitude structural fluctuations of the polypeptide bringing a normally buried chromophore in proximity of the solvent. The latter is an example of protein-gated quenching and the rate is limited by the frequency of the putative conformational transition, υ_g (15). The threshold $kq[Q] \leq \upsilon_g$ predicts the emergence of saturation effects in the Stern-Volmer plot at large $[Q]$. In addition, as Q remains relegated to the aqueous phase, another difference from diffusive penetration is that the rate is rather insensitive to the size of Q.

In the case of AN, there is no evidence of protein-gated quenching, and all available data is consistent with the internal migration mechanism. First, for every protein of this study the lifetime Stern-Volmer plot is linear throughout the AN concentration range investigated (in general up to quenching rates of 1–2 × 10^4 s^{-1}). Second, although the increase in size from AN (mol wt = 53) to acrylamide (mol wt = 71) would hardly slow down the reaction of Trp exposed to the solvent (protein in the open-gate state) it would considerably increase the frictional drag to diffusion of the quencher and reduce significantly kq. In fact, the comparison between AN and acrylamide quenching constants (Fig. 4) shows that, except for GAPDH, kq(acrylamide) is invariably orders of magnitude smaller than kq(AN). As mentioned above, saturation effects on the Stern-Volmer plot have been observed with acrylamide quenching of Cd-azurin (10) and LADH (15), and have been attributed to protein-gated quencher penetration.

We believe that one conclusion from this study is that, in the submillisecond-second timescale of phosphorescence, AN is able to penetrate deeply the inner core of the globular folds. Thus, the quenching rate constant is above all determined by the frictional drag to the diffusion of AN through the polypeptide (D_p) in that, as described by Eq. 4, the thickness of the protein spacer per se has a modest effect on kq. The ratio kq(protein)/kq(NATA) indicates that AN diffusion in proteins is slowed down up to seven orders of magnitude, relative to diffusion in water. Among the proteins examined, kq varies by approximately five orders of magnitude, with a clear trend to decrease with the depth of burial of the triplet probe, even if GAPDH is an exception. The implication is that the flexibility of the polypeptide, as monitored by D_p, drops rapidly toward the interior of the macromolecule. The general increase in $\Delta H^{\pm}(kq)$ with the depth of burial (from 5 to 16 kcal/mol, Table 1) is also indicative that structural fluctuations underlying AN diffusion have higher activation barriers on moving toward the protein interior.

A direct correlation between D_p, as inferred from kq, and the flexibility of the globular fold, is supported by a similar trend exhibited by the oxygen and acrylamide quenching constants of these proteins (Fig. 4). The accessibility of the above quenchers changes in step with that of AN,

even if in absolute terms the overall variation of *kq* is more contained in the case of O_2 and more conspicuous with acrylamide. Other indicators of structural flexibility, such as the intrinsic phosphorescence lifetime (τ_0) and the protein stability to thermal unfolding, emphasize that modulation of *kq* in some of the proteins of Table 1, by either ligand binding or removal of a metal ion, is directly correlated to changes in the dynamical structure of the macromolecule. Thus, *kq*(AN) is reduced 3.5–4-fold in more rigid NAD^+ and ADPR complexes of LADH, whereas it is enhanced approximately twofold in apo-azurin and approximately sevenfold in mdAP, in accord with a greater plasticity expected for these metal-depleted forms. The lack of modulation of *kq* by NAD^+ binding to GAPDH, despite the increased protein stability of the complex would entail a more compact structure, may be related to the unusually high accessibility of Trp^{84} to both AN and acrylamide (Fig. 4). Presumably, in the presence of large channels connecting Trp^{84} to the solvent *kq* is a poor indicator of structural flexibility.

The different range of *kq* values displayed in Fig. 4 for O_2, AN and acrylamide raises the question as to the frequency-amplitude spectrum of protein motions monitored by D_p. To a first approximation D_p provides an integrated, site specific, measure of motions of amplitudes commensurate with the size of *Q* or larger. However, the large increase of D_p from acrylamide to AN and from AN to O_2 implies that *Q* migration is essentially dominated by the smallest amplitude motions compatible with the size of *Q*. In other words, less frequent, larger amplitude structural fluctuations have little additional impact on internal *Q* diffusion. Quenching data indicate that the protein fold is relatively permeable to O_2. D_p drops only one to three orders of magnitude relative to diffusion in water, and it varies by not more than 100-fold from flexible, superficial sites to tight inner cores. Therefore, these small amplitude/high frequency motions seem pervasive of the globular fold and poorly discriminate between flexible and compact regions of the macromolecule. With AN, which is 50% larger than O_2, diffusion in proteins drops from three to seven orders of magnitude, relative to diffusion in water, and the D_p range within the current protein set extends to approximately five orders of magnitude. Thus, structural fluctuations of amplitude that accommodates AN migration are less frequent and, further, become rapidly inhibited in compact cores. In contrast with O_2, the prompt modulation of AN quenching in some proteins also suggests that motions in this amplitude range are much more responsive to changes in structural flexibility. From AN to acrylamide, which is 34% larger, Dp drops further by two to four orders of magnitude. Apparently, structural fluctuations permitting acryl diffusion are comparatively few and, in compact cores (azurin and AP), their frequency may be so small to fall beyond detection in the second timescale. In proteins where acrylamide diffusion is measurable, however, the sensitivity of these large scale motions to changes in protein dynamics proves to be the highest, as emphasized by the largest modulation of *kq* by cofactors binding or metal removal in some proteins of Fig. 4.

In summary, we believe this study has established that neutral AN is a useful short-range quencher of protein phosphorescence. Its size is sufficiently small to penetrate readily even compact protein cores in the timescale of phosphorescence but is suitably large to exhibit appreciable sensitivity to variations in dynamical structure of the globular fold, whether in going from superficial to internal sites or induced by changes in protein conformation. In combination with smaller and larger quenchers, it permits to derive size dependent solute permeability profiles of these macromolecules and to gain information on the frequency-amplitude spectrum of their structural fluctuations.

SUPPORTING MATERIAL

One figure is available at http://www.biophysj.org/biophysj/supplemental/S0006-3495(10)00656-9.

REFERENCES

1. Kale, S., G. Ulas, …, F. Jordan. 2008. Efficient coupling of catalysis and dynamics in the E1 component of *Escherichia coli* pyruvate dehydrogenase multienzyme complex. *Proc. Natl. Acad. Sci. USA.* 105:1158–1163.
2. Persson, E., and B. Halle. 2008. Nanosecond to microsecond protein dynamics probed by magnetic relaxation dispersion of buried water molecules. *J. Am. Chem. Soc.* 130:1774–1787.
3. Eppler, R. K., E. P. Hudson, …, D. S. Clark. 2008. Biocatalyst activity in nonaqueous environments correlates with centisecond-range protein motions. *Proc. Natl. Acad. Sci. USA.* 105:15672–15677.
4. Hammes-Schiffer, S., and S. J. Benkovic. 2006. Relating protein motion to catalysis. *Annu. Rev. Biochem.* 75:519–541.
5. Henzler-Wildman, K., and D. Kern. 2007. Dynamic personalities of proteins. *Nature.* 450:964–972.
6. Bouvignies, G., P. Bernadó, …, M. Blackledge. 2005. Identification of slow correlated motions in proteins using residual dipolar and hydrogen-bond scalar couplings. *Proc. Natl. Acad. Sci. USA.* 102: 13885–13890.
7. Lakowicz, J. R., and G. Weber. 1973. Quenching of protein fluorescence by oxygen. Detection of structural fluctuations in proteins on the nanosecond time scale. *Biochemistry.* 12:4171–4179.
8. Calhoun, D. B., S. W. Englander, …, J. M. Vanderkooi. 1988. Quenching of room temperature protein phosphorescence by added small molecules. *Biochemistry.* 27:8466–8474.
9. Calhoun, D. B., J. M. Vanderkooi, and S. W. Englander. 1983. Penetration of small molecules into proteins studied by quenching of phosphorescence and fluorescence. *Biochemistry.* 22:1533–1539.
10. Cioni, P., and G. B. Strambini. 1998. Acrylamide quenching of protein phosphorescence as a monitor of structural fluctuations in the globular fold. *J. Am. Chem. Soc.* 120:11749–11757.
11. Cioni, P., and G. B. Strambini. 1999. Pressure/temperature effects on protein flexibility from acrylamide quenching of protein phosphorescence. *J. Mol. Biol.* 291:955–964.
12. Saviotti, M. L., and W. C. Galley. 1974. Room temperature phosphorescence and the dynamic aspects of protein structure. *Proc. Natl. Acad. Sci. USA.* 71:4154–4158.

13. Strambini, G. B. 1987. Quenching of alkaline phosphatase phosphorescence by O_2 and NO. Evidence for inflexible regions of protein structure. *Biophys. J.* 52:23–28.

14. Strambini, G. B., and P. Cioni. 1999. Pressure-temperature effects on oxygen quenching of protein phosphorescence. *J. Am. Chem. Soc.* 121:8337–8344.

15. Strambini, G. B., and M. Gonnelli. 2009. Acrylamide quenching of Trp phosphorescence in liver alcohol dehydrogenase: evidence of gated quencher penetration. *Biochemistry.* 48:7482–7491.

16. Vanderkooi, J. M. 1991. Topics in fluorescence spectroscopy. *In* Biochemical Applications. J. R. Lakowicz, editor. Plenum, New York. 113–116.

17. Gonnelli, M., and G. B. Strambini. 2009. No effect of covalently linked poly(ethylene glycol) chains on protein internal dynamics. *Biochim. Biophys. Acta.* 1794:569–576.

18. Tamaki, T. 1981. Sensitization of the phosphorescence of indole through intramolecular energy transfer from the triplet state of covalently linked acetophenone in rigid media at 77 k. *Photochem. Photobiol.* 33:31–34.

19. Karlsson, B. G., T. Pascher, …, L. G. Lundberg. 1989. Expression of the blue copper protein azurin from *Pseudomonas aeruginosa* in *Escherichia coli*. *FEBS Lett.* 246:211–217.

20. Henis, Y. I., and A. Levitzki. 1977. The role of the nicotinamide and adenine subsites in the negative cooperativity of coenzyme binding to glyceraldehyde-3-phosphate dehydrogenase. *J. Mol. Biol.* 117: 699–716.

21. van de Kamp, M., M. C. Silvestrini, …, G. W. Canters. 1990. Involvement of the hydrophobic patch of azurin in the electron-transfer reactions with cytochrome C551 and nitrite reductase. *Eur. J. Biochem.* 194:109–118.

22. Strambini, G. B., and E. Gabellieri. 1991. Phosphorescence from Trp-48 in Azurin - Influence of Cu(Ii), Cu(I), Ag(I), and Cd(Ii) at the Coordination Site. *J. Phys. Chem.* 95:4352–4356.

23. Parker, C. A. 1968. Photoluminescence of Solutions. Elsevier, New York.

24. Strambini, G. B., B. A. Kerwin, …, M. Gonnelli. 2004. The triplet-state lifetime of indole derivatives in aqueous solution. *Photochem. Photobiol.* 80:462–470.

25. Englander, S. W., D. B. Calhoun, and J. J. Englander. 1987. Biochemistry without oxygen. *Anal. Biochem.* 161:300–306.

26. Cioni, P., E. Gabellieri, …, G. B. Strambini. 1994. Heterogeneity of protein conformation in solution from the lifetime of tryptophan phosphorescence. *Biophys. Chem.* 52:25–34.

27. Sillen, A., and Y. Engelborghs. 1998. The correct use of "average" fluorescence parameters. *Photochem. Photobiol.* 65:475–486.

28. Owen, C. S., and J. M. Vanderkooi. 1991. Diffusion-dependent and -independent collisional quenching of fluorescence and phosphorescence. *Comm. Mol. Cell. Biophys.* 7:235–257.

29. Vanderkooi, J. M., S. W. Englander, …, C. S. Owen. 1990. Long-range electron exchange measured in proteins by quenching of tryptophan phosphorescence. *Proc. Natl. Acad. Sci. USA.* 87:5099–5103.

30. Miller, J. R., W. Hartman, and S. J. Abrash. 1982. Long-distance (25Å) electron transfer by triplet excited states in rigid media. *J. Am. Chem. Soc.* 104:4296–4298.

31. Perrin, F. 1924. Law governing the diminution of fluorescent power as a function of concentration. *Compt. Rend.* 178:1978–1980.

32. Lakowicz, J. R., B. Zelent, …, M. L. Johnson. 1994. Distance-dependent fluorescence quenching of tryptophan by acrylamide. *Photochem. Photobiol.* 60:205–214.

33. Marcus, R. A., and N. Sutin. 1985. Electron transfer in chemistry and biology. *Biochim. Biophys. Acta.* 811:265–322.

34. Dexter, D. L. 1953. A theory of sensitized luminescence in solids. *J. Chem. Phys.* 21:836–850.

35. Huddlestone, R. K., and J. R. Miller. 1982. Determination of electron-transfer rate constants from data on tunneling to randomly distributed acceptors in a rigid medium. *J. Phys. Chem.* 86:200–203.

36. Saltiel, J., and B. W. Atwater. 1988. Spin-Statistical Factors in Diffusion-Controlled Reactions. Wiley & Sons, New York.

37. Strambini, G. B., and M. Gonnelli. 1995. Tryptophan phosphorescence in fluid solution. *J. Am. Chem. Soc.* 117:7646–7651.

38. Strambini, G. B., and M. Gonnelli. 1990. Tryptophan luminescence from liver alcohol dehydrogenase in its complexes with coenzyme. A comparative study of protein conformation in solution. *Biochemistry.* 29:196–203.

39. Theorell, H., and K. Tatemoto. 1971. Thermal stability of horse liver alcohol dehydrogenase and its complexes. *Arch. Biochem. Biophys.* 143:354–358.

40. Engeseth, H. R., and D. R. McMillin. 1986. Studies of thermally induced denaturation of azurin and azurin derivatives by differential scanning calorimetry: evidence for copper selectivity. *Biochemistry.* 25:2448–2455.

41. Levashov, P., V. Orlov, …, N. Nagradova. 1999. Thermal unfolding of phosphorylating D-glyceraldehyde-3-phosphate dehydrogenase studied by differential scanning calorimetry. *Biochim. Biophys. Acta.* 1433:294–306.

42. Miller, J. R., J. V. Beitz, and K. R. Huddlestone. 1984. Effect of free energy on rates of electron transfer between molecules. *J. Am. Chem. Soc.* 106:5057–5068.

43. Eftink, M. R. 1991. Topics in fluorescence spectroscopy. *In* Principles. J. R. Lakowicz, editor. Plenum, New York. 53–126.